View metadata, citation and similar papers at core.ac.uk

brought to you by CORE

provided by Drexel Libraries E-Repository and Archives

Proceedings of the 7th International Conference on HydroScience and Engineering

Philadelphia, USA September 10-13, 2006 (ICHE 2006)

ISBN: 0977447405

Drexel University

College of Engineering

Drexel E-Repository and Archive (iDEA)
http://idea.library.drexel.edu/

Drexel University Libraries
www.library.drexel.edu

The following item is made available as a courtesy to scholars by the author(s) and Drexel University Library and may contain materials and content, including computer code and tags, artwork, text, graphics, images, and illustrations (Material) which may be protected by copyright law. Unless otherwise noted, the Material is made available for non profit and educational purposes, such as research, teaching and private study. For these limited purposes, you may reproduce (print, download or make copies) the Material without prior permission. All copies must include any copyright notice originally included with the Material. **You must seek permission from the authors or copyright owners for all uses that are not allowed by fair use and other provisions of the U.S. Copyright Law.** The responsibility for making an independent legal assessment and securing any necessary permission rests with persons desiring to reproduce or use the Material.

Please direct questions to archives@drexel.edu

INITIAL TESTS OF A NEW COMUPATIONAL LINEARIZATION METHOD

Shipeng Fu[1] and Ben Hodges[2]

ABSTRACT

The 2D shallow water equations (SWE) have been widely used in hydraulic science and engineering. Numerical discretization based on midpoint rule (e.g. leapfrog method) is desirable for 2nd order temporal accuracy. However, the explicit 3-level Leapfrog approach must be applied with appropriate strategies to decouple the known instability mode (Peyret and Taylor, 1983). In this paper, we propose a "Time-Centered, Split-Implicit" (TCSI) method based on a 2-level midpoint rule. This new method computationally linearizes the advection term such that individual solution steps are implicit and linear, but their combination is discretely equivalent to nonlinear midpoint rule discretization. To verify the capability of the new method, the 2D SWE are used to develop and test the TCSI approach. Test cases of simulating a standing wave in a closed basin are performed to examine a variety of model characteristics.

1. INTRODUCTION

The Leapfrog method, based on midpoint rule, is popular in meteorology and oceanography (Fujima and Shigemura 2000). The typical leap-frog approach is a three-level method, discretized as

$$\phi^{n+1} = \phi^{n-1} + f\left(\phi^n \phi^n, \phi^n\right)\Delta t + O(\Delta t^3) \tag{1}$$

where f is a function of a nonlinear advection term ($\phi^n\phi^n$) and a diffusion term (ϕ^n). The midpoint rule is a desirable discretization as it has second-order temporal accuracy. However, the explicit Leapfrog approach must be applied with appropriate strategies to decouple the known instability mode (Peyret and Taylor, 1983). We would prefer a two-level method based on the midpoint rule that can be written as

$$\phi^{n+1} = \phi^n + f\left(\phi^{n+1/2}\phi^{n+1/2}, \phi^{n+1/2}\right)\Delta t + O(\Delta t^3) \tag{2}$$

which has the desirable property that the time n+1/2 information is retained only within the computation of the n to n+1 time step, and does not directly appear in the discrete equation for n+3/2 time step. If the n+1/2 values in eq. 2 are further discretized by the linear approximation

[1] Graduate Student, Department of Civil, Architectural, and Environmental Engineering, University of Texas at Austin, Austin, TX 78712, USA (shipengfu@mail.utexas.edu)

[2] Associate Professor, Department of Civil, Architectural, and Environmental Engineering, University of Texas at Austin, Austin, TX 78712, USA (hodges@mail.utexas.edu)

$\phi^{n+1/2} = \left(\phi^n + \phi^{n+1}\right)/2$, the resulting equation is both implicit and nonlinear, which is generally not a good starting point for a numerical method. However, below we introduce a new splitting method based on exactly this form. This new method computationally linearizes the advection term such that individual solution steps are implicit and linear, but their combination is discretely equivalent to nonlinear eq. 1. We call this a "Time-Centered, Split-Implicit" (TCSI) method.

1.1 Computational Linearization

To solve a nonlinear equation system, computational linearization techniques are typically the most effective approach. One example is the local time-linearization method (e.g. Lomax, Pulliam and Zingg, 1996). In local time-linearization, an implicit nonlinear term (e.g. $\phi^{n+1}\phi^{n+1}$), is approximated with information from the known and unknown time steps (e.g. $\phi^n\phi^{n+1}$) by using a Taylor-series expansion. The resulting equation retains the nonlinear term, but time-lagging one variable provides a linear equation set for time-integration. However, use of $\phi^n\phi^{n+1}$ to represent $\phi^{n+1}\phi^{n+1}$ provides first-order temporal accuracy. The new TCSI approach is similar to local-time linearization, but is formally second-order accurate in time by using a two-step approach.

The TCSI method applies the approximation

$$\phi^{n+1/2} = \frac{\phi^n + \phi^{n+1}}{2} + O\left(\Delta t^2\right) \tag{3}$$

Substituting eq. 3 into eq. 2 for one of the advective terms provides:

$$\phi^{n+1} = \phi^n + f\left\{\left[\frac{\phi^n + \phi^{n+1}}{2} + O\left(\Delta t^2\right)\right]\phi^{n+1/2}, \phi^{n+1/2}\right\}\Delta t + O(\Delta t^3) \tag{4}$$

which can be written as:

$$\phi^{n+1} = \phi^n + f\left(\phi^n\phi^{n+1/2}, \phi^{n+1}\phi^{n+1/2}, \phi^{n+1/2}\right)\frac{\Delta t}{2} + O(\Delta t^3) \tag{5}$$

Thus the nonlinear advection term is discretely linearized without losing the original accuracy.

1.2 Computational Splitting

Observing that eq. 5 has two different nonlinear terms, a computational splitting approach can be applied:

$$\phi^* = \phi^n + f\left(\phi^n\phi^{n+1/2}, \phi^{n+1/2}\right)\frac{\Delta t}{2} \tag{6}$$

$$\phi^{n+1} = \phi^* + f\left(\phi^{n+1}\phi^{n+1/2}, \phi^{n+1/2}\right)\frac{\Delta t}{2} + O(\Delta t^3) \tag{7}$$

where ϕ^* is an intermediate solution and substituting eq. 6 into eq. 7 returns eq. 5. To create a solvable system, it can be shown that

$$\phi^{n+1/2} = \phi^{*} + O\left(\frac{\Delta t}{2}\right)^{2} \tag{8}$$

so that we are free to substitute ϕ^{*} for $\phi^{n+1/2}$ on the RHS of eq. 6 and eq. 7 without affecting the overall accuracy. With this substitution, the original split system becomes:

$$\phi^{*} = \phi^{n} + f\left(\phi^{n}\phi^{*}, \phi^{*}\right)\frac{\Delta t}{2} + O(\Delta t^{3}) \tag{9}$$

$$\phi^{n+1} = \phi^{*} + f\left(\phi^{n+1}\phi^{*}, \phi^{*}\right)\frac{\Delta t}{2} + O(\Delta t^{3}) \tag{10}$$

Eq. 9 and eq. 10 are two implicit linear steps of a general time-centered split-implicit (TCSI) method that is formally second-order temporally accurate for nonlinear evolution equations. Solution with second-order spatial differences will result in each step being a simple tridiagonal inversion.

2. IMPLEMENTATION AND TESTING FOR 2D SHALLOW WATER EQUATIONS

2.1 Discretized Equation

We use the 2D shallow water equation to develop and test the TCSI approach. The 2D shallow water equations can be written as:

$$\frac{\partial U}{\partial t} + U\frac{\partial U}{\partial x} + V\frac{\partial U}{\partial y} = -g\frac{\partial \zeta}{\partial x} + \nu\left(\frac{\partial^{2} U}{\partial x^{2}} + \frac{\partial^{2} U}{\partial y^{2}}\right) \tag{11}$$

$$\frac{\partial V}{\partial t} + U\frac{\partial V}{\partial x} + V\frac{\partial V}{\partial y} = -g\frac{\partial \zeta}{\partial y} + \nu\left(\frac{\partial^{2} V}{\partial x^{2}} + \frac{\partial^{2} V}{\partial y^{2}}\right) \tag{12}$$

$$\frac{\partial H}{\partial t} + \frac{\partial HU}{\partial x} + \frac{\partial HV}{\partial y} = 0 \tag{13}$$

$$\zeta = H + Z_{b} \tag{14}$$

where U and V are depth-averaged velocities in x and y directions; g is the gravitational acceleration; H is the water depth and ζ is surface elevation; Z_b is the bottom elevation. The above statement of the 2D SWE neglects the turbulence closure and bottom stress as a test case to our numerical method,

Applying the midpoint rule between time 'n' and n+1' along with central-differencing of spatial derivatives on an Arakawa C grid (Arakawa and Lamb, 1977), eqs. 11, 12 and 13 can be discretized as a set of coupled nonlinear equations:

$$\begin{aligned}\frac{U_{i,j+1/2}^{n+1} - U_{i,j+1/2}^{n}}{\Delta t} = {} & -U_{i,j+1/2}^{n+1/2}\frac{\left(U_{i,j+3/2}^{n+1/2} - U_{i,j-1/2}^{n+1/2}\right)}{2\Delta x} - V_{i,j+1/2}^{n+1/2}\frac{\left(U_{i+1,j+1/2}^{n+1/2} - U_{i-1,j+1/2}^{n+1/2}\right)}{2\Delta y} \\ & + \frac{\nu}{\Delta x^{2}}\left(U_{i,j-1/2}^{n+1/2} - 2U_{i,j+1/2}^{n+1/2} + U_{i,j+3/2}^{n+1/2}\right) + \frac{\nu}{\Delta y^{2}}\left(U_{i-1,j+1/2}^{n+1/2} - 2U_{i,j+1/2}^{n+1/2} + U_{i+1,j+1/2}^{n+1/2}\right) \\ & - \frac{g}{\Delta x}\left(\zeta_{i,j+1}^{n+1/2} - \zeta_{i,j}^{n+1/2}\right)\end{aligned} \tag{15}$$

$$\frac{V_{i+1/2,j}^{n+1}-V_{i+1/2,j}^{n}}{\Delta t}=-U_{i+1/2,j}^{n+1/2}\frac{\left(V_{i+1/2,j+1}^{n+1/2}-V_{i+1/2,j-1}^{n+1/2}\right)}{2\Delta x}-V_{i+1/2,j}^{n+1/2}\frac{\left(V_{i+3/2,j}^{n+1/2}-V_{i-1/2,j}^{n+1/2}\right)}{2\Delta y}$$
$$+\frac{\nu}{\Delta x^{2}}\left(V_{i+1/2,j-1}^{n+1/2}-2V_{i+1/2,j}^{n+1/2}+V_{i+1/2,j+1}^{n+1/2}\right)+\frac{\nu}{\Delta y^{2}}\left(V_{i-1/2,j}^{n+1/2}-2V_{i+1/2,j}^{n+1/2}+V_{i+1/2,j}^{n+1/2}\right) \quad (16)$$
$$-\frac{g}{\Delta y}\left(\zeta_{i+1,j}^{n+1/2}-\zeta_{i,j}^{n+1/2}\right)$$

$$\frac{H_{i,j}^{n+1}-H_{i,j}^{n}}{\Delta t}=-\frac{1}{\Delta x}\left(H_{i,j+1/2}^{n+1/2}U_{i,j+1/2}^{n+1/2}-H_{i,j-1/2}^{n+1/2}U_{i,j-1/2}^{n+1/2}\right)-\frac{1}{\Delta y}\left(H_{i+1/2,j}^{n+1/2}V_{i+1/2,j}^{n+1/2}-H_{i-1/2,j}^{n+1/2}V_{i-1/2,j}^{n+1/2}\right) \quad (17)$$

2.2 Discussion and Results of Simulating a Standing Wave in a Closed Basin

As a test of the TCSI method, a free surface standing wave in a rectangular basin has been simulated for the basin shown in Figure 1. An equally-spaced 20×5 mesh is used. It is recognized that the model mesh and initial conditions provide essentially a 1D exercise that does not fully test the x-y decoupling of the method; however, this mesh does allow testing of how the method treats the nonlinear $u\partial u/dx$ term. Free-slip boundary conditions are enforced on all walls and the bottom.

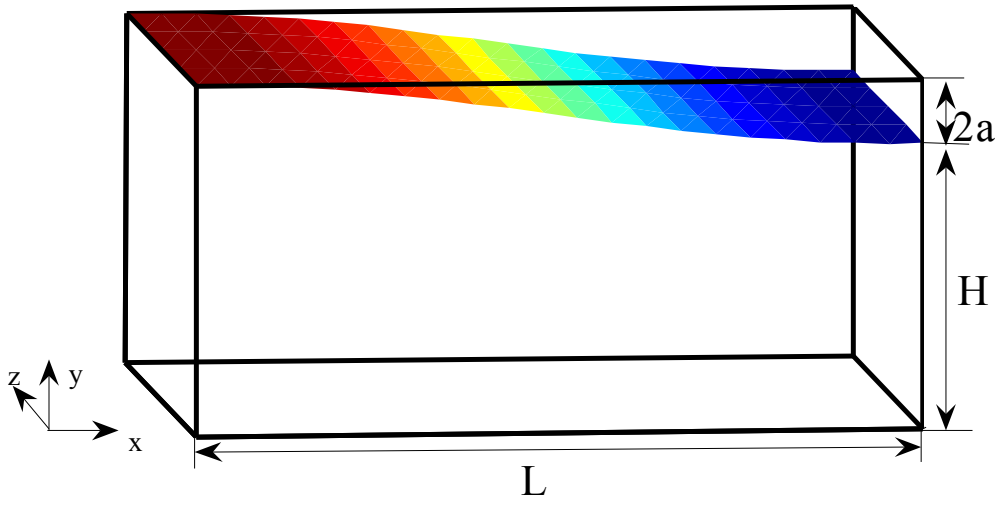

Figure 1 A standing wave in a rectangular basin

The period of an inviscid free surface wave is (Dean and Dalrymple 1998):

$$T=\sqrt{\frac{2\pi\lambda}{g}\left(\tanh kH\right)^{-1}} \quad (18)$$

where 'T' is the wave period; 'λ' is the wave length; 'k' is the wave number and 'H' is the water depth. According to linear wave theory, the wave function is a sinusoid for small amplitude waves. The surface height (h) above the still water level is:

$$h(x,t)=a\sin\left(kx\right)\sin\left(\sigma t\right) \quad (19)$$

where the frequency (σ) is $2\pi/T$; 'a' is the free surface wave amplitude. For a viscous unconfined wave in deep water, the evolution of the wave amplitude can be approximated as (Lamb 1932),

$$a(t) = a(0)e^{-2\nu k^2 t} \tag{20}$$

where 'ν' is kinematic viscosity and 'k' is the wave number. However, wave damping based on eq. 20 is unlikely to be well-represented in a 2D depth-averaged model as vertical velocity and vertical velocity shears are part of the closure term. The Reynolds number is defined as:

$$\mathrm{Re} = \frac{Lu}{\nu} \tag{21}$$

where L is the length of the basin, ν is the kinematic viscosity and u is the characteristic Cartesian fluid velocity based on the wave amplitude (a) and the wave frequency (σ):

$$u = a\sigma \tag{22}$$

We have run simulations for different cases to examine a variety of model characteristics. To find out how out model perform in different ratios of water depth to basin length (i.e. H/L), three different cases are tested and compared in Figure 2. Furthermore, three simulations with different initial wave steepness (i.e. ratio of wave amplitude to basin length) are presented in Figure 3. All the six simulations are run in an inviscid flow to exclude viscous damping effects. Results in Figure 2 and Figure3 illustrate the nondimensionalized water surface elevation (i.e. $(\zeta - H)/a$) at $x = \Delta x/2$, which is the grid cell center closest to the left wall. The important parameters for these six test cases are listed in Table 1.

Table 1 Parameters of simulations of a standing wave

case	H/L	a/L	Re	L/λ
3a	0.05	5.0×10^{-4}	∞	0.5
3b	0.1	5.0×10^{-4}	∞	0.5
3c	0.2	5.0×10^{-4}	∞	0.5
4a	0.05	5.0×10^{-4}	∞	0.5
4b	0.05	2.0×10^{-3}	∞	0.5
4c	0.05	5.0×10^{-3}	∞	0.5

In Figure 2, three cases with different H/L ratio are compared. As the water depth increases, the simulation wave period is shortened. The wave dispersion behavior of this method requires further research.

In Figure 3, we compare waves with different initial steepness. Wave steepening is inherently a nonlinear effect, which increases with increasing initial amplitude, thus we do not expect agreement between linear theory and. As the SWE governing equations retain nonlinearity but neglect non-hydrostatic dispersion, the wave steepening will be greater. Moreover, we keep the nonlinearity while the hydrostatic approximation is inherent in SWE. This two facts will introduce additional steepening (Hodges et al. 2006). In case 4a, a very small initial wave steepness is introduced and the simulation show little nonlinear effects. With the initial steepness increased in case 4b and 4c, the nonlinear effects are more and more obvious.

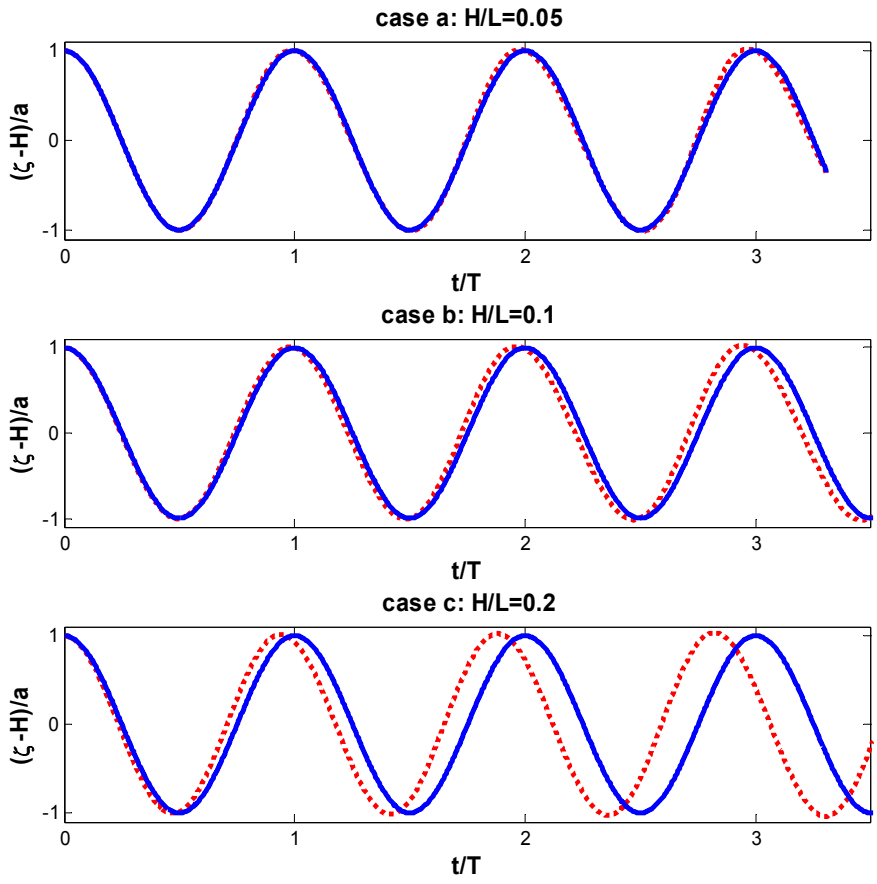

Figure 2 Modeled water surface elevation at x=0 for different ratios of H/L with small amplitude wave (a/L = 5 x 10^{-4}) and inviscid model. ——— analytical solution, ------- simulation.

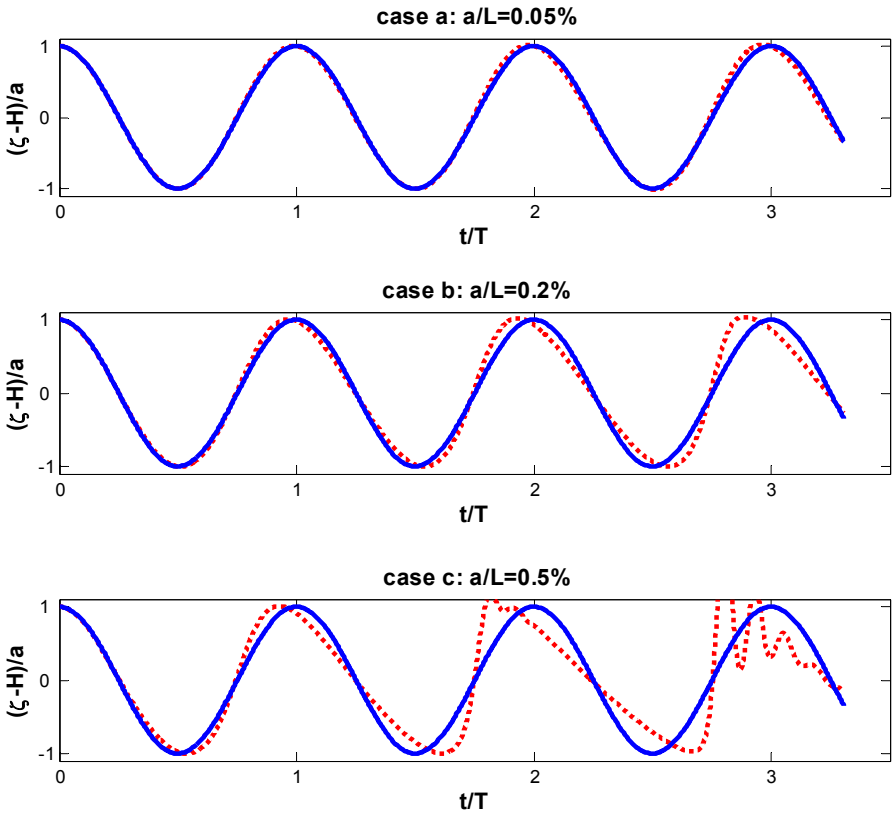

Figure 3 Modeled water surface elevation at x=0 for different ratios of a/L in shallow water (H/L = 0.05) with inviscid model. ——— analytical solution, ·····simulation.

Figure 4 (below) displays results for a viscous simulation. Walls and boundaries are free slip, so the only viscous terms are wave-induced (rather than wave-boundary induced). The Reynolds number is equal to 0.1. Our simulation result damped slower than the analytical solution, eq. 20. This result is not unexpected because that 2D SWE neglect the velocity gradients in the vertical (i.e. $\partial u / \partial z = 0$). As a result, the viscous damping due to $\nu \partial^2 u / \partial z^2$ is not reflected in our simulation. Thus, 2D SWE cannot correctly represent the damping of a standing wave without an additional modeling term to represent the viscous term which is partially lost in the depth averaging process.

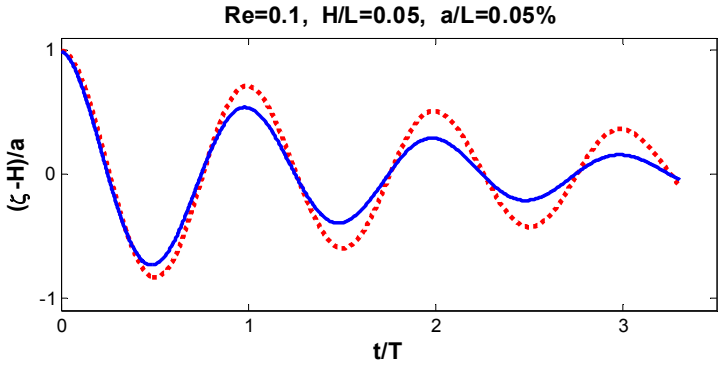

Figure 4 Viscous simulation results. ——— analytical solution, ·····simulation.

REFERENCES

Arakawa, A., and Lamb, V.R. (1977). "Computational design of the basic dynamical processes of the UCLA general circulation model", Methods in Computational Physics, vol.17, Academic Press, New York, 173-265.

Dean, R.G. and Dalrymple, R.A. (1998). Water Wave Mechanics for Engineering and Scientists, World Scientific Publishing Co. Pte. Ltd., New Jersey.

Fujima, K. and Shigemura, T. (2000). "Determination of Grid Size for Leap-Frog Finite Difference Model to Simulate Tsunamis around A Conical Island", Costal Engineering, vol42, No.2, pp. 197-210.

Hodges, B.R., Laval, B., and Wadzuk, B.M. (2006). "Numerical error assessment and temporal horizon for internal waves in a hydrostatic model", Ocean Modeling Vol. 13, No. 1, pp. 44-64.

Lamb, H. (1932). Hydrodynamics. Cambridge University Press.

Lomax, H., Pulliam, T.H. and Zingg, D.W. (1996) Fundamentals of Computational Fluid Dynamics. Springer, New York Inc.

Peyret, R. and Taylor, T.D. (1983). Computational Method s for Fluid Flow. Springer-Verlag, New York Inc.